

How Well Do Regional Climate Models Reproduce Radiation and Clouds in the Arctic? An Evaluation of ARCMIP Simulations

MICHAEL TJERNSTRÖM AND JOSEPH SEDLAR

Department of Meteorology, Stockholm University, Stockholm, Sweden

MATTHEW D. SHUPE

Cooperative Institute for Research in Environmental Sciences, University of Colorado, and NOAA/Earth System Research Laboratory, Boulder, Colorado

(Manuscript received 3 August 2007, in final form 21 January 2008)

ABSTRACT

Downwelling radiation in six regional models from the Arctic Regional Climate Model Intercomparison (ARCMIP) project is systematically biased negative in comparison with observations from the Surface Heat Budget of the Arctic Ocean (SHEBA) experiment, although the correlations with observations are relatively good. In this paper, links between model errors and the representation of clouds in these models are investigated. Although some modeled cloud properties, such as the cloud water paths, are reasonable in a climatological sense, the temporal correlation of model cloud properties with observations is poor. The vertical distribution of cloud water is distinctly different among the different models; some common features also appear. Most models underestimate the presence of high clouds, and, although the observed preference for low clouds in the Arctic is present in most of the models, the modeled low clouds are too thin and are displaced downward. Practically all models show a preference to locate the lowest cloud base at the lowest model grid point. In some models this happens also to be where the observations show the highest occurrence of the lowest cloud base; it is not possible to determine if this result is just a coincidence. Different factors contribute to model surface radiation errors. For longwave radiation in summer, a negative bias is present both for cloudy and clear conditions, and intermodel differences are smaller when clouds are present. There is a clear relationship between errors in cloud-base temperature and radiation errors. In winter, in contrast, clear-sky cases are modeled reasonably well, but cloudy cases show a very large intermodel scatter with a significant bias in all models. This bias likely results from a complete failure in all of the models to retain liquid water in cold winter clouds. All models overestimate the cloud attenuation of summer solar radiation for thin and intermediate clouds, and some models maintain this behavior also for thick clouds.

1. Introduction

Although anthropogenic climate change is a global issue, climate change is most pronounced in the Arctic. The current warming trend in the Arctic is about 2 times that of the global average (MacBean 2004; Serreze and Francis 2006) and is projected to continue through this century (Kattsov and Källén 2004; Holland and Bitz 2003). Arctic climate change has therefore

come to the forefront of climate science during the last decade (see, e.g., Arctic Climate Impact Assessment 2005). Despite much attention, there is still no consensus on specific reasons why climate change is accelerated in the Arctic, although several hypotheses have been suggested (see, e.g., Arctic Climate Impact Assessment 2005). In an interdisciplinary study, Overpeck et al. (2005) concluded that the Arctic system is “heading toward a new super-interglacial state.” They find that the current trajectory of the Arctic climate system suggests this new state will be characterized by substantially less permanent ice and snow, which will have far-reaching effects on animal, plant, and human life. They also conclude that there are no obvious or currently

Corresponding author address: Michael Tjernström, Department of Meteorology, Stockholm University, SE-106 91 Stockholm, Sweden.
E-mail: michael@misu.su.se

TABLE 1. Summary of participating models. For vertical grid system type, “Z” indicates a geometric system and “P” indicates a system based on pressure; different scaling may have been applied to account for terrain height. For the cloud schemes, ARCSYM, COAMPS, and Polar MM5 use separate prognostic equations for solid vs liquid, cloud water, and precipitation. HIRHAM, RCA, and REMO carry a single equation for cloud water, determine liquid and ice fractions based on temperature, and analyze all precipitation in each column of the model at each time step; SW is for shortwave and LW is for longwave radiation.

Model name, Name of responsible group	Vertical grid			Time step (min)
	No. (total/below 500 m)	Lowest level (m)	Type	
ARCSYM University of Colorado	23/4	35–40	P	2.5
COAMPS Stockholm University	30/7	15	Z	1.5
HIRHAM Alfred-Wegener Institute	19/3	25–30	P	5
Polar MM5 University of Colorado	23/4	30–50	P	2.5
RCA Swedish Meteorological and Hydrological Institute	24/3	70–85	P	30
REMO Max-Planck Institute for Meteorology	20/3	55–65	P	5

well-understood feedbacks within the Arctic system that can reverse or even slow this development.

Cloud feedback effects lie at the heart of this discussion, yet cloud modeling remains a challenge in today’s climate models. Sensitivity to cloud processes is identified as the main uncertainty in climate modeling (Stainforth et al. 2005; Solomon et al. 2007). Clouds have a major impact on the radiation budget at the surface and on the climate system as a whole; thus, it is vital to assess how models handle the description of clouds. Clouds are subgrid-scale features in models and therefore must be parameterized. Although different models employ unique cloud parameterizations, each is typically based on empirical evidence, usually from data collected at lower latitudes. Several studies suggest that Arctic cloud processes are not always identical to those at lower latitudes. For example, Intrieri et al. (2002) found a sizeable fraction of clouds containing liquid water, even in the cold Arctic winter, which have a potentially large effect on the surface longwave radiation (Shupe and Intrieri 2004; Prenni et al. 2007). Moreover, summertime studies indicate a low number concentration of cloud condensation nuclei (CCN) in the Arctic (Covert et al. 1996; Heintzenberg et al. 2006), affecting the shortwave optical properties of the clouds.

A major problem when assessing parameterizations in global models is the nonlinear behavior of the climate system and its many degrees of freedom. It is therefore difficult to compare details among models. Model climates will tend toward different states on many scales, thereby making comparisons of model errors and feedbacks difficult. These complexities make direct comparisons to single-point observations almost impossible. Regional climate modeling is a very powerful tool in both these contexts. By prescribing ana-

lyzed lateral boundary conditions, the same large-scale meteorological context can be imposed in many models. Using a reasonably small model domain, regional models are constrained to follow a particular large-scale flow for a particular time period, facilitating comparisons with specific site observations and among models.

Within the Arctic Regional Climate Model Intercomparison Project (ARCMIP; Curry and Lynch 2002; <http://curry.eas.gatech.edu/ARCMIP/index.html>) framework, Rinke et al. (2006) compared the adherence of the large-scale flow patterns in different models with the forcing analyses. Tjernström et al. (2005, hereinafter TEA05) investigated the model performance for the surface heat fluxes in the Arctic using the same model runs. Both papers conclude that the regional models remain reasonably faithful to the large-scale flow; however, TEA05 found significant problems with the surface energy balance. Although the turbulent heat fluxes showed only a small annual bias, they also included very large random and systematic errors. Turbulent heat fluxes were typically overestimated, regardless of sign, and were poorly correlated to observations. A near-zero annual bias thus resulted from a cancellation of large positive and negative random errors. The radiation fluxes, in contrast, showed relatively good correlations with the observations, but instead suffered from significant persistent biases.

This study focuses on downwelling radiation at the surface and its relation to modeled cloud properties. The surface net radiation balance additionally depends on the surface temperature and surface albedo, adding a complex error interaction. The focus on downwelling radiation in this study is an attempt to isolate the impact of clouds on surface radiation. It can be argued

TABLE 1. (Extended)

Prognostic moist variables (No./type)	Cloud scheme reference	Radiation scheme reference	Effective radius (liquid/ ice) (μm)	Main model reference
4/ice and liquid, cloud and precipitation	Hsie et al. (1984)	Hack et al. (1993); Mlawer et al. (1997)	10(SW) 7(LW)/40	Lynch et al. (1995)
4/ice and liquid, cloud and precipitation	Rutledge and Hobbs (1983)	Harshvardhan et al. (1987)	5–45/10–60	Hodur (1997)
1/total cloud water	Roeckner et al. (1996)	Roeckner et al. (1996)	4–24/12–80	Christensen et al. (1996)
4/ice and liquid, cloud and precipitation	Reisner et al. (1998)	Hack et al. (1993)	10/14.6	Cassano et al. (2001)
1/total cloud water	Rasch and Kristjánsson (1998)	Sass et al. (1994)	4–24/15–80	Jones et al. (2004)
1/total cloud water	Roeckner et al. (1996)	Roeckner et al. (1996)	4–24/12–80	Jacob (2001)

that multiple reflections between clouds and a surface of snow and ice are important (Wyser et al. 2008). The observed downwelling shortwave radiation has a contribution from radiation reflected by the bottom of the cloud that has already having been reflected at least once from the surface. An error in surface temperature is also likely to have an impact on the temperature of low clouds (TEA05) and thus on the downwelling longwave radiation. It is very difficult to determine how these processes are handled in different models, and focusing on downwelling radiation is a first step toward understanding how clouds affect the energy balance at the Arctic surface in these models.

2. The ARCMIP program

ARCMIP aims to identify model deficiencies and to improve the description of Arctic climate processes in numerical models through controlled regional model experiments. The strategy is to use regional models to improve global climate modeling. In a regional model, the larger-scale climate is controlled (or forced) by prescribing the lateral boundaries from global analyses. Systematic errors in the regional models that are not due to the forcing are likely attributed to deficiencies in their description of subgrid-scale processes (i.e., the parameterizations). The higher spatial resolution in a regional model than in a global model allows for a better representation of important feedback processes. Four previous papers (TEA05; Rinke et al. 2006; Inoue et al. 2006; Wyser et al. 2008) describe various aspects of the model intercomparison experiment.

The first ARCMIP experiment is a 13-month-long simulation of the western Arctic, from September 1997 through September 1998, in coordination with the year-long Surface Heat Budget of the Arctic Ocean (SHEBA;

Uttal et al. 2002) field program. All models (see Table 1) were set up on a common domain over the western Arctic, using the same target resolution of about 50 km. Vertical resolutions and numerical details were different in each model. Lateral boundary forcing was provided at 6-h intervals using European Centre for Medium-Range Weather Forecasts (ECMWF) operational analyses. Ice and sea surface temperature (SST) and ice fraction were prescribed from Advanced Very High Resolution Radiometer (AVHRR) and Special Sensor Microwave Imager (SSM/I) satellite observations, respectively. The surface temperature over land was derived from each model's surface energy balance calculations. One additional run with the Coupled Ocean–Atmosphere Mesoscale Prediction System (COAMPS) model also used a simplified parameterization for the energy balance at the ice surface (this run is referred to as “COAMPS Ice”). It is worth emphasizing that all simulations were run continuously through the whole year without the benefit of data assimilation, essentially allowing systematic errors to grow. However, the analyses on the lateral boundaries from ECMWF are taken from a data assimilation cycle in which soundings and surface observations from SHEBA were ingested.

The models have different cloud parameterizations falling into two main categories (see Table 1). Three of the models [COAMPS, the Arctic Regional Climate System Model (ARCSYM), and the polar version of the fifth-generation Pennsylvania State University–National Center for Atmospheric Research Mesoscale Model (Polar MM5)] carry separate prognostic equations for solid and liquid water phases of both cloud and precipitation. HIRHAM [HIRHAM derives from its parent models, the High-Resolution Limited-Area Model (HIRLAM) and the Max Planck Institute for Meteorology GCM ECHAM, which itself is derived

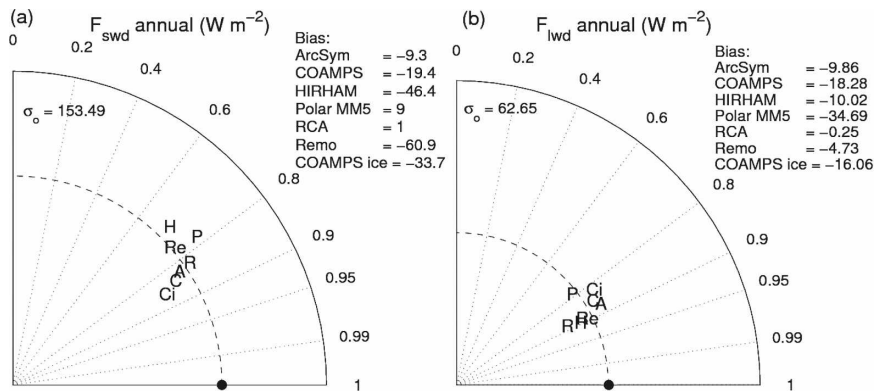


FIG. 1. Taylor diagrams showing modeled errors in downwelling (a) shortwave and (b) longwave radiation ($W m^{-2}$) at the surface for the whole SHEBA year. The different models are represented by the first letter in the model name, except for REMO (Re) and COAMPS Ice (Ci). The distance from the origin denotes the std dev of each model normalized by the observed std dev, also given in the top left of each plot. The black dot on the abscissa denotes the std dev of the observations normalized by itself (i.e., unity), which is where a perfect model would lie. The angle to the abscissa denotes the cosine of the correlation coefficient to the observations. Also given in the top right of each plot is the annual bias for each model.

from models at ECMWF and Deutsches Klimarechenzentrum, Hamburg], the Rossby Center Atmospheric Model (RCA), and the German Weather Service regional model (REMO) carry only a single cloud water variable and distinguish between cloud ice and liquid using empirical temperature relationships. The latter three also release all precipitation in each model column during every model time step and do not allow for precipitation to be advected or to be stored in the column between time steps. See TEA05 for a discussion of other aspects of the models.

All model results were output every 3 h and were compared with observations from the SHEBA (Uttal et al. 2002) experiment. The radiation data are from the Atmospheric Surface Flux Group (ASFG) instrumented tower (Persson et al. 2002); also used are data from radiosoundings performed throughout the year (C. Bretherton and S. de Roode 2006, personal communication). Cloud observations are from surface-based remote sensing observations described in Intrieri et al. (2002), mainly from microwave radiometry, cloud radar, and lidar (see Moran et al. 1998; Alvarez et al. 1998). Cloud boundaries were analyzed directly from the output from these instruments; the cloud liquid and ice water paths come from retrievals applied to these remote sensing observations described in Shupe et al. (2005, 2006). The estimated error in the derived cloud liquid water path (LWP) is ± 25 $g m^{-2}$, and the uncertainty in the ice water path (IWP) is substantially larger but also more difficult to assess; about a factor of ± 2 is a reasonable estimate (Shupe et al. 2005).

3. Results

a. Radiation

Figures 1–3 summarize the downwelling radiation errors in all models; an error is defined as model results minus observations. For the shortwave radiation (Fig. 1a), only data for which the sun is more than 10° above the horizon are used. Figure 1, based on 3-hourly data for the whole year utilizing the Taylor diagram¹ concept (Taylor 2001), confirms conclusions from TEA05 that correlations between modeled and observed radiation are relatively high and RMS errors are relatively small. The shortwave radiation correlations to observations are relatively good in all models, ~ 0.7 – 0.9 . Moreover, the modeled variability is also roughly

¹ In a Taylor diagram, the agreement between two datasets (here, modeled and observed time series) is described by an angle and a radius in a polar coordinate system. The angle is given by $\varphi = \cos^{-1}(r)$, where r is the correlation coefficient between the datasets, which is also displayed on the outer circle of the diagram. The length of the radius a is determined by the standard deviation. All standard deviations are normalized by the observed standard deviations. The black dot on the abscissa represents the observations: it lies on the unity circle because the standard deviation of the observations divided by itself is unity, and on the abscissa ($\varphi = 0$) because the correlation coefficient of the observations to itself is unity. Simple trigonometry shows that the straight distance between this dot and a point representing a model result is proportional to the model RMSE. Multiple possible combinations of correlation and variability may thus cause a given RMSE. Results from a perfect model would lie on the black dot; farther distances from this dot indicate poorer model results.

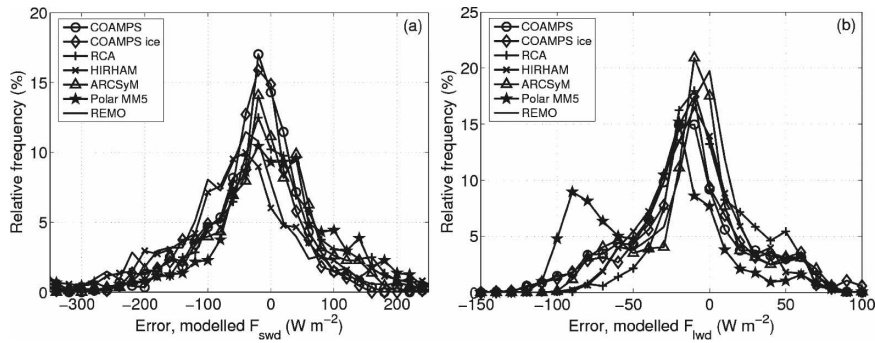


FIG. 2. Relative PDFs of the modeled errors in downwelling (a) shortwave and (b) longwave radiation at the surface ($W m^{-2}$). Longwave radiation is calculated for the whole SHEBA year; shortwave radiation is only calculated for times when the solar zenith angle is smaller than 80° .

correct, as indicated by the clustering of all models on the (dashed) unity radius. RCA and Polar MM5 have a very small positive annual bias; the rest of the models have a negative bias, with the largest in REMO, followed by HIRHAM and COAMPS Ice. The longwave radiation results (Fig. 1b) are even more closely grouped with correlations ranging from 0.8–0.9, but here the annual bias is negative in all models, although small in RCA and REMO. The largest error is found in Polar MM5, followed by both COAMPS runs. Figure 2, using the same data, shows the annual error probability

density functions (PDFs) for all models. These usually peak at negative values, from approximately -40 to $-20 W m^{-2}$ for the shortwave and from approximately -25 to $0 W m^{-2}$ for longwave radiation; the PDF for longwave radiation in Polar MM5 has an unexpected bimodal distribution.

Resolved in time using weekly averages for the 1998 summer season (Fig. 3), the error in incoming solar radiation is the smallest early and late in the season, with peaks of surplus solar radiation at times in spring and autumn when the sun starts and stops being impor-

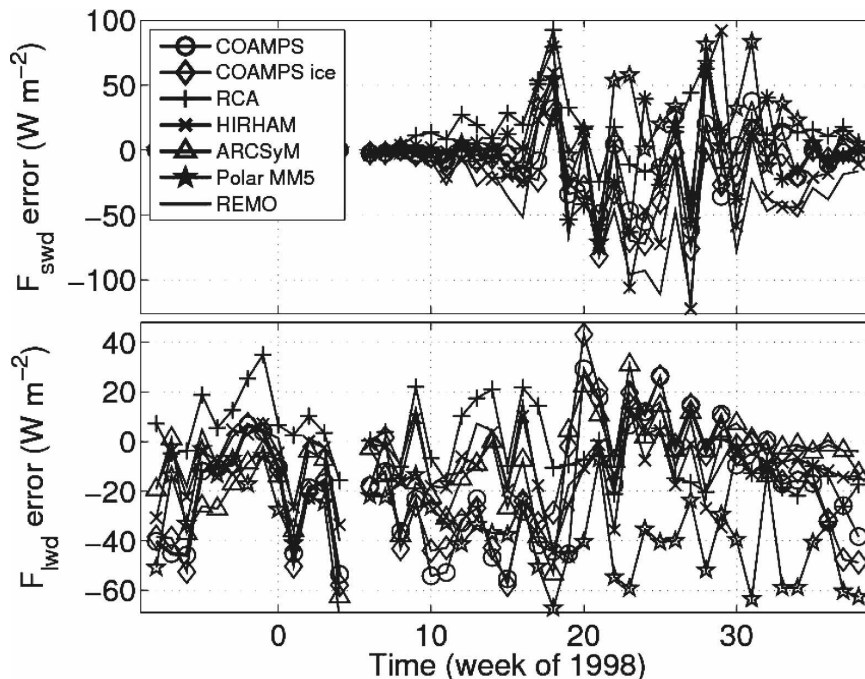


FIG. 3. Time series of the weekly averaged modeled errors in downwelling (top) shortwave and (bottom) longwave radiation at the surface ($W m^{-2}$) for the whole SHEBA year. For shortwave radiation, only the summer of 1998 is shown. The gap in the longwave record results from instrument problems.

tant for the surface energy balance. Between these times, roughly weeks 18–27 of 1998, the model errors are scattered between 0 and -100 W m^2 . During these midsummer weeks, Polar MM5 and RCA have the smallest errors, sometimes positive and sometimes negative, and REMO has the largest negative error; the remaining models are scattered around $\sim -50 \text{ W m}^2$. For longwave radiation, data from the entire experiment are used. There is, for some unknown reason, a distinct difference between the autumns of 1997 and 1998. From October 1997 until that end of the year, the error is negative in all models except RCA, between 0 and -50 W m^2 . After a gap in the data (due to insufficient observations to form weekly averages) the models group into two regimes: RCA, REMO, HIRHAM, and ARCSYM with a smaller negative error and both COAMPS runs and Polar MM5 with a larger negative error. The RCA error is in general close to 0; Polar MM5 has the largest negative error. About 20 weeks into 1998, which is early in the melt season, the model errors become smaller and very similar to each other, except for in Polar MM5 where the error remains as earlier, $\sim -50 \text{ W m}^2$. It is also worth noting that the time period when the shortwave deficit is the largest (weeks 18–28) is also a period when the longwave radiation error is, on average, slightly positive (except for in Polar MM5 and HIRHAM). These biases are consistent with an overprediction of cloud optical thickness during summer, leading to both excess longwave emission and shortwave attenuation. For the total radiation at the surface, the shortwave and longwave effects are partially offsetting.

Considered over the full year, the model ensemble average error represents a substantial deficit in incoming radiation at the surface, which in a coupled model system would have a detrimental effect on the melting and freezing of sea ice. Note, however, that among the different models errors in downwelling surface radiation balance may or may not be offset by, for example, compensating errors in surface albedo or temperature. Individual models may therefore still provide reasonable results for other parameters, although possibly for the wrong reasons. There is no reason to expect that such compensating errors should remain in balance for a changing climate, for example if the Arctic should become ice-free in summer, as suggested by several models (e.g., Arctic Climate Impact Assessment 2005).

b. Cloud representation

Because clouds play a major role in determining the radiation at the surface, it is expected that systematic model biases in the surface downwelling radiation may be caused by the model representation of clouds, the

cloud–radiation interaction, or both. Evaluating an annual cycle of modeled cloud water content is complicated because that property is difficult to robustly observe. Thus, here we focus on comparisons of observed and modeled cloud geometry, column-integrated quantities such as liquid and ice water paths, and on longer-term statistics rather than on one-to-one correspondence.

1) CLOUD GEOMETRY

In the model data, thresholds of cloud water content, regardless of phase, determine cloud boundaries. The observed cloud geometry is based on thresholds of lidar and radar reflectivity, and are also independent of phase and do not distinguish cloud from precipitation. Some differences between models and observations may thus be artifacts of defining these thresholds differently.

The relative frequency of cloud-base height for the lowest observed and modeled clouds is presented in Fig. 4. Observations indicate a lowest cloud base (LCB) most often near 100 m, higher than in the majority of models. However, the lowest-level observations ($\leq 100 \text{ m}$) are impacted by different, and sometimes variable, minimum observation heights by the lidar and radar. Thus, some observations at these levels may be biased high, and the strong peak at 100 m is likely overestimated at the expense of the lower levels. The highest frequency of LCB for RCA and REMO is $\sim 100 \text{ m}$, which happens to be the height of the first vertical model level in these models (see Table 1), possibly making this agreement fortuitous. Both COAMPS runs, ARCSYM, and Polar MM5 seem to favor lower LCBs but also have higher model resolution near the surface. The COAMPS runs suggest a tendency for either very low cloud bases ($\sim 15 \text{ m}$) or a cloud base slightly higher than 500 m. A similar trend is found for Polar MM5 and HIRHAM except the second maximum is higher, near 2 km. Most models have a tendency to underestimate the frequency of LCBs in the middle to upper troposphere. Winter and summer LCB frequencies are also included in Fig. 4. In winter, both COAMPS runs, ARCSYM, and RCA indicate cloud bases nearly always at their first model level, compensated by a significant underestimation of the frequency of higher LCBs, especially in COAMPS. Apart from an overestimation of low-level cloud bases in winter, HIRHAM and REMO broadly agree with observations. Polar MM5 has very few occasions with low cloud bases in winter but has a reasonable occurrence of higher cloud bases. During summer, REMO and RCA continue to simulate LCBs most often at the first model level. Both COAMPS runs suggest a significant reduc-

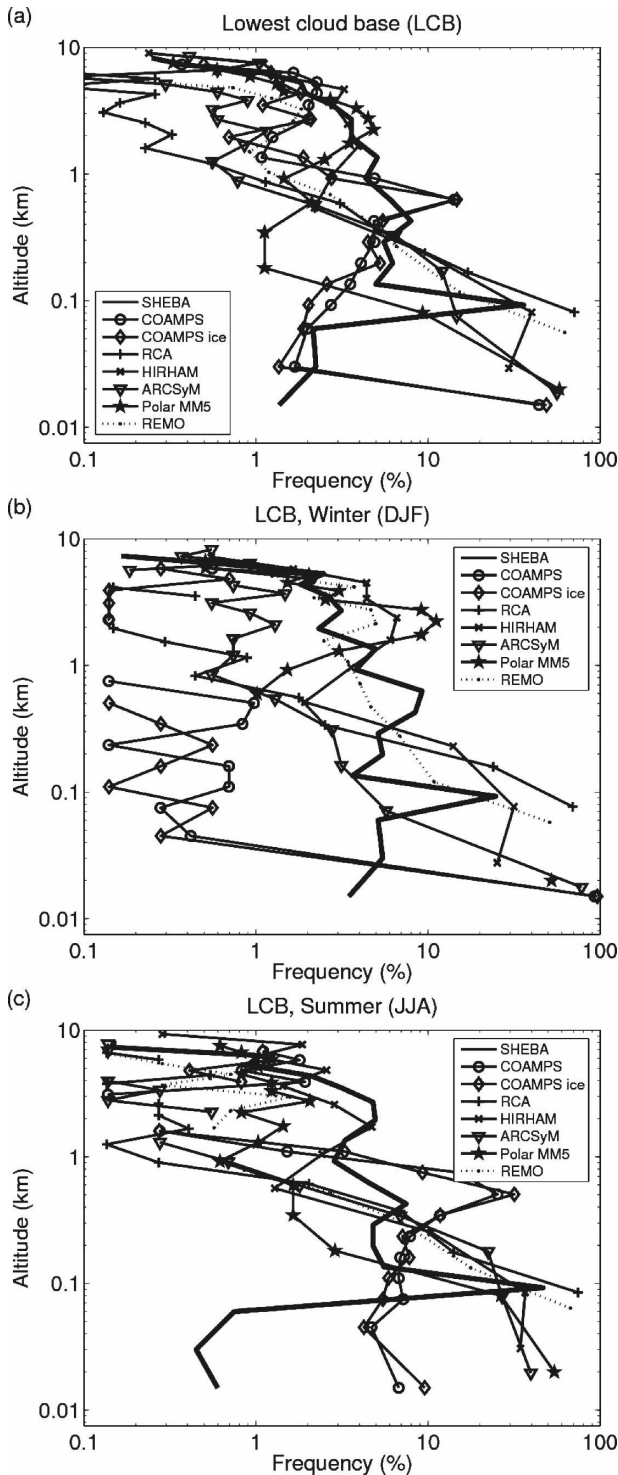


FIG. 4. PDFs for the lowest cloud-base height in meters for all models for (a) the whole SHEBA year and for (b) winter and (c) summer.

tion of the occurrence of LCB at the first vertical model level, compensated by elevated LCBs at ~ 500 m. All models except HIRHAM underestimate the occurrence of high LCBs.

The frequency of occurrence of the lowest cloud-top height is restricted to single-layer clouds (see Fig. 5a). It is apparent that all models overestimate the occurrence of lowest cloud tops (LCTs) below 700 m and vice versa at higher altitudes. Observations of LCTs (which were not expected to be biased due to range gate heights) indicate LCTs occurred most often between ~ 800 m and ~ 2 km. Because the LCBs were most often observed near 100 m (Fig. 4a), this indicates common relatively thick low-level clouds during the SHEBA year. Although models do tend to simulate very low cloud bases, the preference for lower LCTs leads to single-layer low-level clouds that are too thin and possibly systematically displaced downward. Throughout the free troposphere, simulated LCTs typically occur less frequently than observed; models favor single cloud layers confined to lower levels. Observations indicate lower cloud tops during winter with a slight increase during summer. Models show a similar trend, particularly in ARCSYM and Polar MM5.

The highest observed and modeled cloud top heights, regardless of number of cloud layers, are shown in Fig. 5b. Observations indicate a quasi-constant relative frequency of highest cloud tops (HCTs) through 0.7–7 km, with the largest values near 7 km. The majority of models capture the relative maximum of occurrence in HCT near 7 km; HIRHAM overestimates the occurrence of cloud tops at this altitude and ARCSYM underestimates it. Lower in the atmosphere, all models simulate an overabundance of HCTs below ~ 500 m; ARCSYM, RCA, and REMO simulate their respective HCT frequency maxima below roughly 200 m.

The frequency of observed and modeled numbers of cloud layers is shown in Fig. 6. Before discussing these results, it is worthwhile to note differences in how cloud layering is modeled and observed. In the models, layers are defined using cloud water, excluding precipitation; the layering only takes into account the clouds themselves. In the observations, this distinction between cloud and precipitation is difficult to make. Thus, two or more layers of clouds with precipitation falling between and through them will often be observed as one layer. It would therefore be natural to expect cases with multilayer precipitating clouds to contribute to a bias in the observations toward fewer observed cloud layers. The observations indicate that single-layer clouds were observed most often but that two cloud layers also occurred frequently. All models, except Polar MM5, also

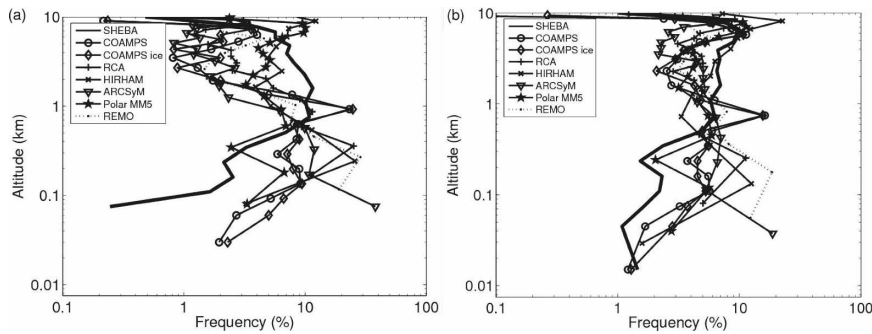


FIG. 5. As in Fig. 4, but for the (a) lowest single-layer cloud top and (b) highest cloud top for the whole SHEBA year.

show a preference for one or two cloud layers, in broad agreement with the observations (e.g., Intrieri et al. 2002). Polar MM5 indicates a maximum frequency of 0 (cloud free) or a single cloud layer. Both COAMPS runs and RCA have significantly lower occurrences of clear skies. The majority of models have a somewhat larger frequency of more than two cloud layers; both COAMPS runs, ARCSYM, and RCA more often simulate multiple cloud layers than are observed. Recall, however, that fewer cases observed with several cloud layers may be an artifact of the observational technique (see discussion above). Overall, HIRHAM and REMO cloud-layer statistics conform well to the observations in this context.

2) CLOUD WATER

Figure 7 shows the error analysis of modeled cloud water paths again using Taylor diagrams. Neither the liquid- nor ice-water path is well simulated with any of the models in terms of correlations or RMSE, although the correlation for the liquid-water path, at 0.2–0.5, is slightly higher than for the ice-water path, at <0.3. The modeled LWP variability relative to the observations, at 0.5–2, is higher than for IWP, which is systematically low, at 0.1–1. Although the annual bias in LWP can be either negative or positive among the models, it is consistently negative for IWP, except for in RCA. As expected from the strong annual temperature cycle in the Arctic (e.g., TEA05), there is a substantial annual cycle in LWP (Fig. 8a) of more than an order of magnitude. Nonetheless, all models manage to overestimate this cycle because although all models have a reasonable LWP in summer, they all underpredict LWP in winter. In fact, all three models with more sophisticated moist physics have no liquid water in winter; the three models employing a simpler scheme predict some liquid but still much too little. In summer, COAMPS and ARCSYM temporarily overpredict LWP, but also have long periods with quite reasonable results; however,

Polar MM5 consistently underpredicts cloud liquid. IWP, in contrast, has a much weaker annual cycle (Fig. 8b) in both observations and models. However, the IWP magnitude is very different in the different models. Given the large uncertainty in the observations, ARCSYM consistently underpredicts IWP, and COAMPS and Polar MM5 underpredict IWP in summer. RCA has marginally high values, mostly during the summer half of the year. There is a high degree of IWP variability between days 0 and 60 that appears to be well captured by a few of the models.

Figure 9a shows PDFs of total cloud water path (CWP, liquid plus ice) for models and SHEBA observations. The models tend to overpredict, sometimes by a factor of 2, the frequency of low CWP events. In contrast, the frequency of cases with $50 \text{ g m}^{-2} < \text{CWP} < 400 \text{ g m}^{-2}$ is too low for all models except in RCA. Polar MM5 significantly underestimates the frequency of cases with $\text{CWP} > \sim 50 \text{ g m}^{-2}$, with the opposite bias for very small CWPs. Defined as a $\text{CWP} < 0.1 \text{ g m}^{-2}$, cloud-free conditions almost never occur in

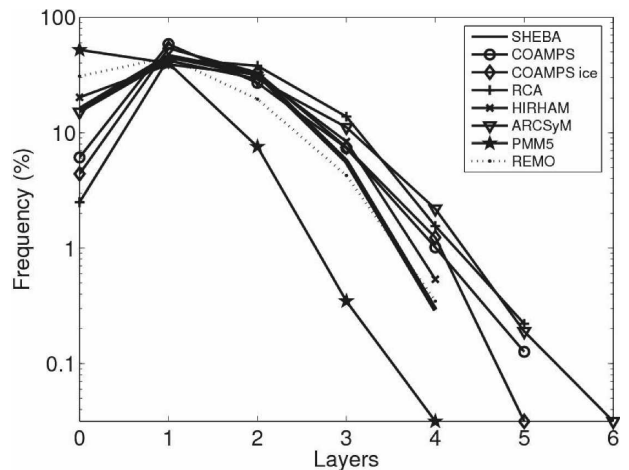


FIG. 6. PDFs of the number of cloud layers in the observations and model simulations for the whole SHEBA year.

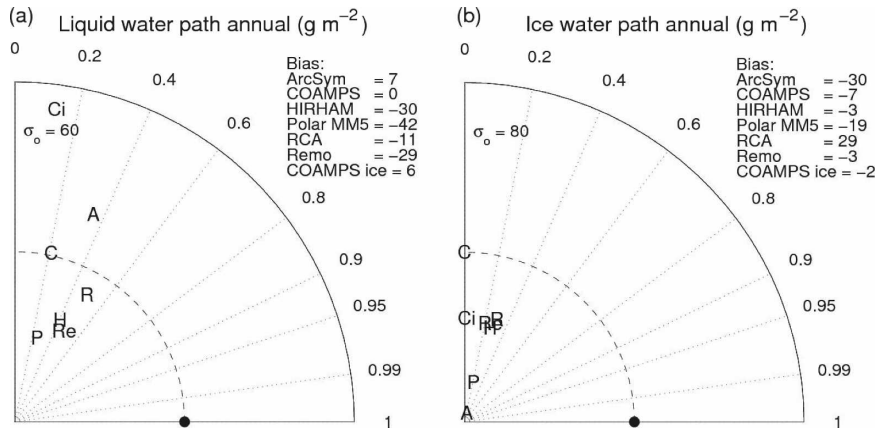


FIG. 7. As in Fig. 1, but for the (a) LWPs and (b) IWPs (g m^{-2}) for the whole SHEBA year.

RCA and occur much too often in Polar MM5 (also see the cloud layer statistics in Fig. 6), but the other models seem more reasonable. Figures 9b and 9c demonstrate how these results are related to cloud water phase. Most of the models agree well with the observations of IWP for moderate and low values, but the PDFs for IWP fall off too rapidly at higher values (Figs. 9b). For LWP, almost all models underestimate the occurrence of moderate and high values (Figs. 9c), but both COMAPS runs and ARCSYM overestimate the frequency of the very largest values.

ARCSYM, Polar MM5, and RCA deviate significantly from the observations, but in different ways. ARCSYM severely underestimates the occurrence of cloud ice at any amount; Polar MM5 severely underestimates occasions with high IWP. Polar MM5 also underestimates LWP over the whole range, leading to a pronounced underestimation of total cloud water. RCA overestimates the frequency of moderate IWPs but underestimates the frequency of the lowest and the highest IWPs. These discrepancies explain most of this model's deviation from the observed CWP.

There are also differences in how each model distributes water between ice and liquid. Figure 10 shows the annual PDFs of the fraction of LWP to total CWP when clouds are present. Note that a fraction lower than unity does not necessarily indicate mixed-phase clouds; simultaneous nonzero values of LWP and IWP can result from liquid and ice clouds at different altitudes. An underestimation of, for example, cirrus clouds with a reasonable estimation of stratocumulus may thus manifest itself into a fraction that is too high. The observations have a rather flat PDF, with liquid water somewhat more often dominating over ice. Polar MM5 closely follows this behavior; all the other models have significant deviations. Note, however, the systematic underestimation of both liquid and ice cloud water by Polar MM5 shown in Figs. 8 and 9; this is thus a case of good agreement for the wrong reasons. The two remaining models with separate prognostic equations for ice and liquid, COAMPS and ARCSYM, tend to almost always have much more liquid than ice and very seldom more ice than liquid. All three models with a single total cloud water prognostic equation have the

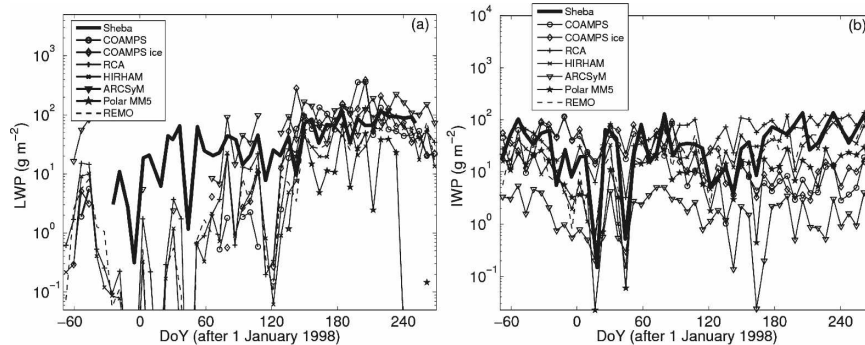


FIG. 8. Time series of weekly averaged (a) LWP and (b) IWP (g m^{-2}) from all models and the observations.

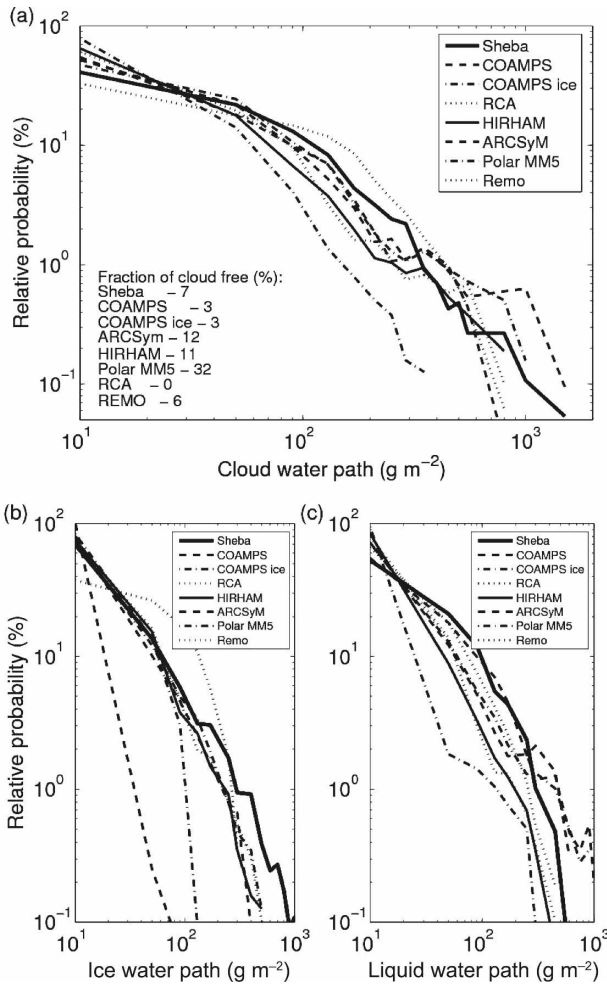


FIG. 9. PDFs of the (a) total CWPs (b) IWPs, and (c) LWPs (g m^{-2}) for the whole SHEBA year.

opposite behavior; IWP dominates more often while LWP seldom dominates.

Errors in modeled clouds may emerge due to errors in available moisture. Figure 11 shows model biases in integrated water vapor (IWV) from SHEBA soundings and how they relate to cloud water. Clearly there is a similar intermodel behavior in IWV errors (Fig. 11a), with a near-zero or slightly positive model bias for low values ($\text{IWV} < \sim 7\text{--}8 \text{ kg m}^{-2}$), typically during winter, and pronounced negative errors for larger ones ($\text{IWV} > 12 \text{ kg m}^{-2}$), typically during summer. The largest intermodel differences occur for $\text{IWV} > 15 \text{ kg m}^{-2}$, with the largest error in ARCSYM from approximately -4 to -6 kg m^{-2} and the smallest in REMO from only approximately -2 to -4 kg m^{-2} . Even larger biases appear for IWV approaching 20 kg m^{-2} ; these are omitted here due to a very small number of occurrences. It is not clear what is causing these errors. The amount of water in the vertical column of any regional model is a

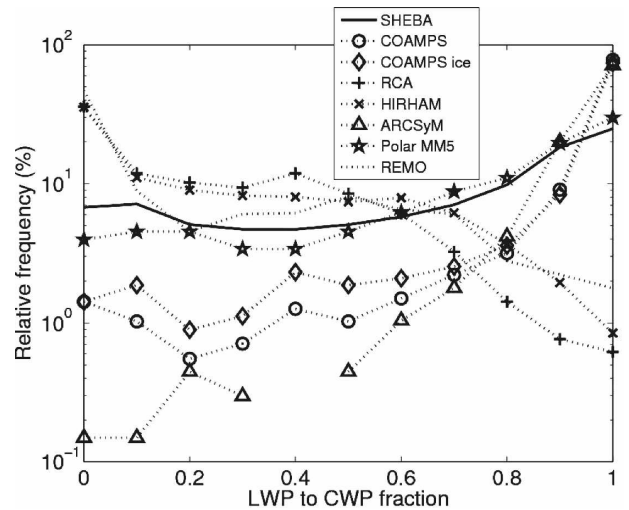


FIG. 10. PDFs of the ratio of the LWP to the total CWP for the whole SHEBA year.

balance between what is forced upon the model at the lateral boundaries, surface moisture flux, condensation to clouds, and loss by precipitation. In each model, the description of moist processes is tuned together with all the other physical processes to provide an optimal performance, usually measured by some large-scale property such as top-of-the-atmosphere radiation or forecast skill for the 500-hPa height. This tuning, while necessary, may introduce compensating errors. Thus, each model has its own unique “model climate,” which differs among the models and from reality in subtle ways. It is expected that a regional model whose moist parameterization is substantially different from that in the global model used to generate the lateral boundary conditions will react by redistributing water between different reservoirs. A model with a somewhat dry climate compared to the lateral boundary forcing may, for example, react by producing excess precipitation to rid itself of the “perceived” excess water. Here we compare model results to soundings, making it impossible to judge how much of the error is already present in the boundary conditions from the ECMWF model that is forcing the regional models. Certainly, the very largest errors, at the highest IWVs, likely come either from the boundary forcing fields or from errors in the soundings. The decreasing frequency as IWV increases makes it difficult to identify the reason for the error. However, the systematic and increasing negative bias as IWV increases past approximately $12\text{--}13 \text{ kg m}^{-2}$ seems to suggest that the problem might lie in the interaction with the boundary-forcing fields from the ECMWF analysis.

Figure 11b shows the mean LWP for each model and the observations as a function of the IWV; all cases were used regardless of the presence of clouds. As ex-

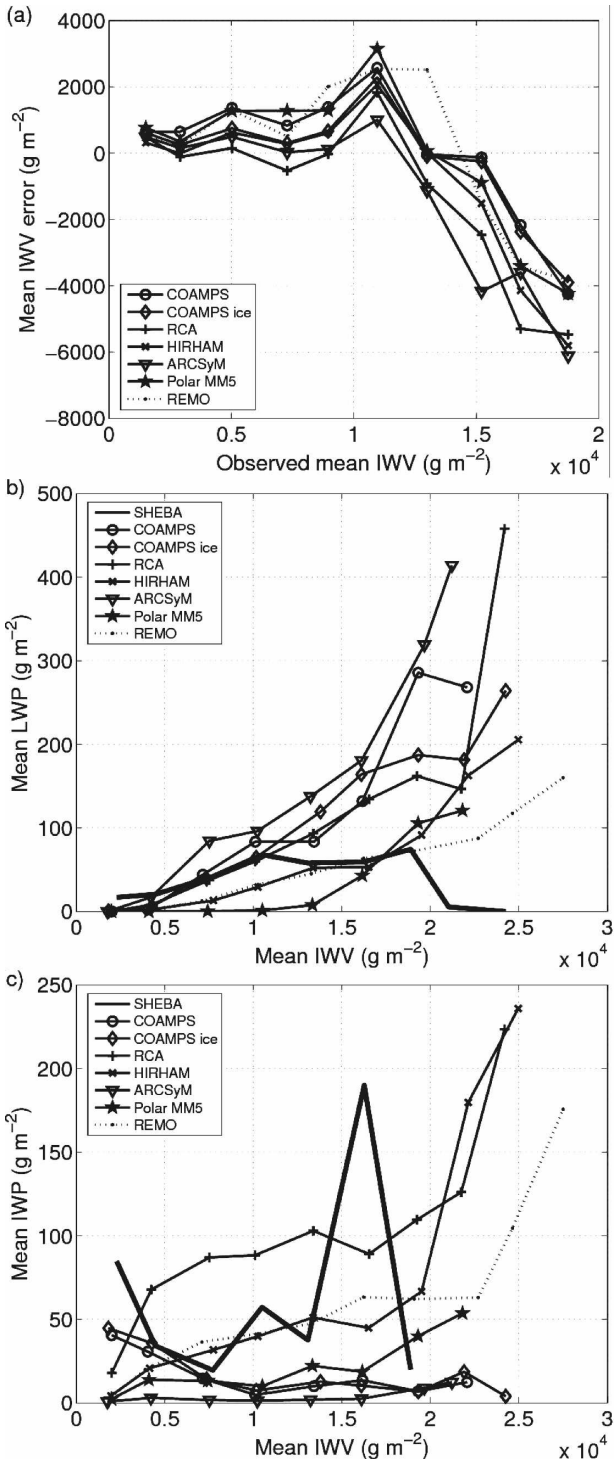


FIG. 11. Plots of (a) the mean error (model – observations) of the IWV (g m^{-2}) as a function of its observed value, and (b) LWPs and (c) IWPs (g m^{-2}) as a function of the IWV for the whole SHEBA year.

pected, a dryer atmosphere (low IWV) gives rise to less dense liquid-water clouds (low LWP) and vice versa. It also seems that the actual values of LWP for a given IWV are much higher than in the observations for most models, except for the very thinnest clouds. It is interesting to note that the model with the largest IWV error (most underpredicted IWV) for any given observed value (i.e., ARCSYM) is also the model with the largest LWP for that IWV. The opposite is also true; the model with the smallest IWV error (i.e., REMO) tends to have the lowest LWP at high IWV. One may therefore speculate that errors in IWV result partly from a tendency in some models to form liquid clouds more easily than other models. This error should be the most important in summer when the IWV is large, which is at least partly supported by Fig. 3. A similar correlation between modeled IWP and IWV is, however, not obvious (Fig. 11c). Models with a large LWP for a given IWV do not necessarily also have a large IWP or vice versa, although ARCSYM and both COAMPS runs seem to have the largest LWP and the lowest IWP for a given IWV.

Although we do not attempt to utilize observational data for the height distribution of cloud water, it is informative to compare how the different models distribute the cloud water vertically. Figure 12 shows the probability of cloud water (liquid plus ice) for all the models as a function of height (COAMPS Ice is not shown because it is nearly identical to COAMPS). Several similarities and differences can be identified. Clouds are frequently simulated within the lowest few hundred meters, which is consistent with Arctic observations (Intrieri et al. 2002; Tjernström et al. 2004). However, the frequency of cloud water (CW) through the first 300 m illustrates intermodel differences. COAMPS tends to have fewer and less dense low-level clouds that are somewhat evenly distributed with height. The ARCSYM low-level CW distribution shows a strong decrease with altitude, suggesting a preference for shallow and thin low clouds. REMO and RCA have a similar CW distribution to COAMPS, but with much higher frequencies, suggesting more frequent thicker and denser low-level clouds. HIRHAM shows a relative minimum in CW at the lowest model levels, with a maximum near 200 m. Polar MM5 also has a CW maximum through the lowest levels, with an abrupt cutoff at 0.015 g kg^{-1} . All models, except Polar MM5, show lower CW around 1 km, but the thickness of this minimum varies between models. Polar MM5, as an exception, has a dramatically different structure with a peculiar maximum stretching from the low levels up through the midtroposphere; this explains its results in Fig. 9c. This distribution has a cutoff-like upper limit indicating

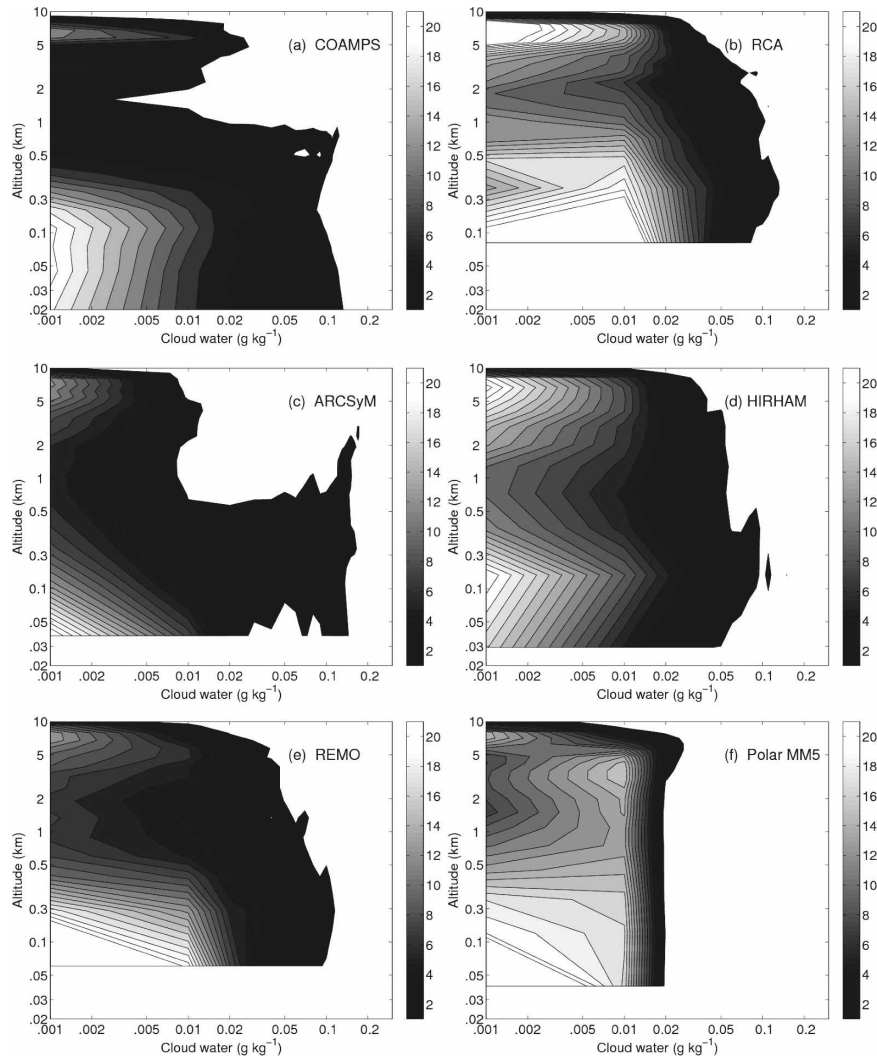


FIG. 12. Contour plots of the probability of occurrence for total cloud water content (g kg^{-1}) as a function of height for (a) COAMPS, (b) RCA, (c) ARCSYM, (d) HIRHAM, (e) REMO, and (f) Polar MM5.

an artificially fast transfer of cloud water to precipitation for higher values of CW. Polar MM5 also has a minimum of occurrences of cloud-free conditions through 1–5 km. Common to all models are clouds appearing in the upper free troposphere, between approximately 5 and 8 km. A significant difference among models, however, is the frequency of occurrence of these clouds. COAMPS has the lowest occurrence with the lowest CW values; ARCSYM, REMO, and Polar MM5 also have low values of CW but at a higher frequency; Polar MM5, HIRHAM, and RCA have higher probabilities of high CW above 2–5 km. There are also notable differences in the seasonal behavior among the models (not shown).

Errors in CW and cloud geometry both contribute to

errors in CWP; however, observations of cloud water content in all cloud types for long periods are difficult to obtain. An attempt is made here to estimate the mean liquid water content using a combination of LWP and cloud geometry for single-layer liquid clouds; only clouds with a top below 2 km were used. Figure 13 shows that for mean cloud liquid water content below 60 g m^{-3} , the scatter between the models is substantial. HIRHAM does reasonably well, but REMO and RCA overestimate and COAMPS, Polar MM5, and ARCSYM underestimate the frequency of small values. The models agree well for higher values but tend to overestimate their frequency. This indicates that when clouds are present in these models, they are too seldom thin clouds (especially in COAMPS and ARCSYM),

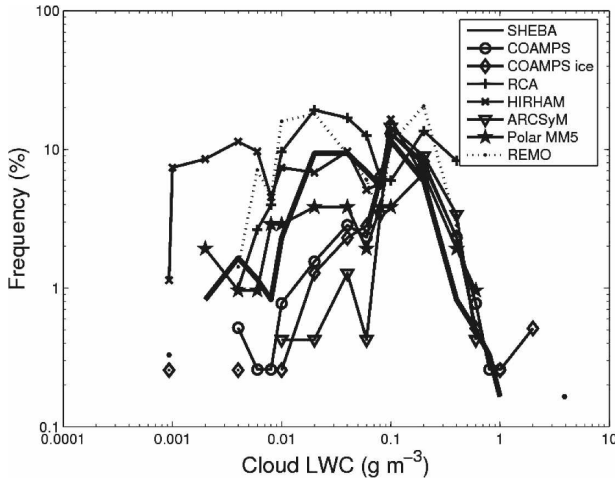


FIG. 13. PDF of the mean liquid water content (g m^{-3}) from the models and the observations for single-layer liquid water clouds with cloud tops below 2 km. In the models, this is calculated directly from the model output; from the observations, it is calculated from the cloud boundaries and the LWP.

but occurrence of thick clouds is more realistic. Note, however, that this analysis is valid only for single-layer liquid clouds and that the implication for radiation errors on a seasonal time scale is difficult to interpret.

c. The cloud–radiation interaction

Cloud-related radiation errors can result either from an erroneous simulation of the clouds (too little or too much, at the wrong altitude, or with the wrong phase) or from errors in the way the cloud–radiation interaction itself is described. Even perfectly simulated clouds are not sufficient if their impact on the radiation is described erroneously.

Figure 14 shows PDFs of radiation errors split into cloudy and clear situations for winter and summer, here defined as November–April and May–September, respectively. For shortwave radiation (Fig. 14a), only summer is considered. Clear and cloudy situations are distinguished based on thresholds in the total cloud water path. Somewhat arbitrarily, cloud-free conditions are here assumed for $\text{CWP} < 5 \text{ g m}^{-2}$; $\text{CWP} > 20 \text{ g m}^{-2}$ is considered cloudy. Varying these values within reason has only small consequences for the results. In con-

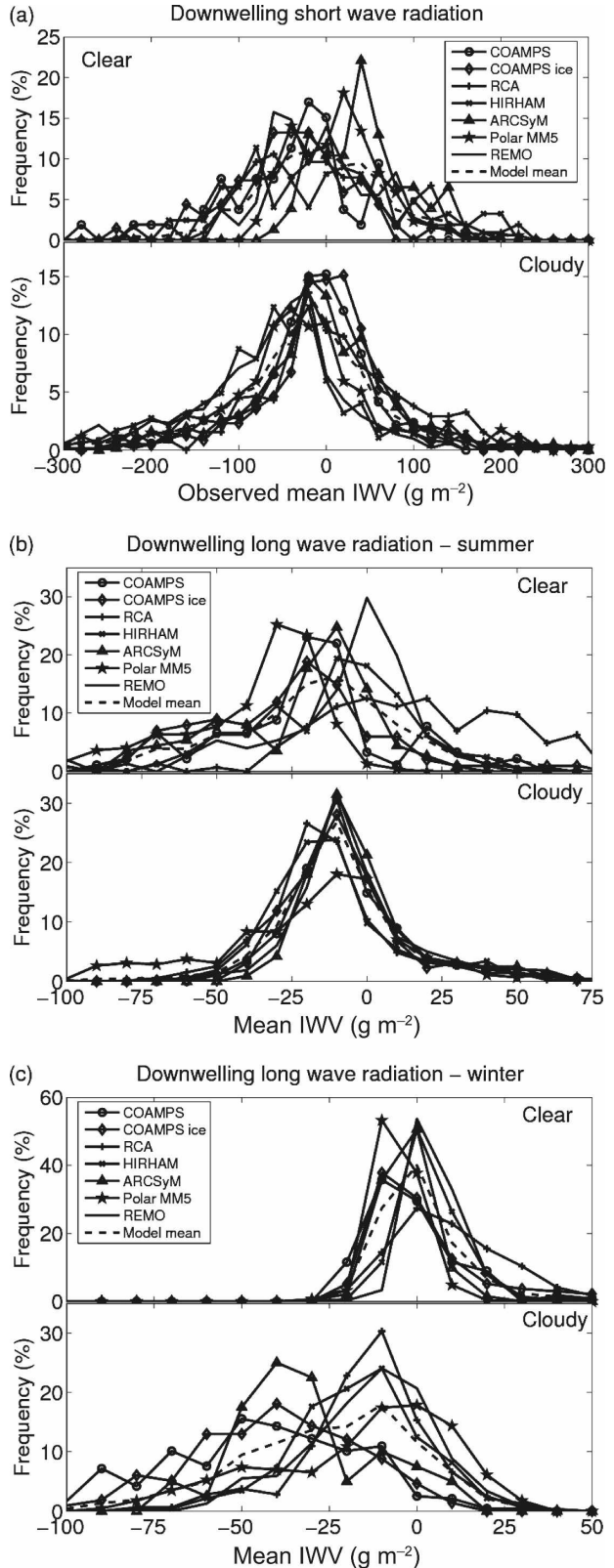


FIG. 14. PDFs of the model errors in (a) shortwave and (b) longwave radiation for summer 1998 and (c) longwave radiation for the 1997/98 winter season (W m^{-2}). The results are divided into clear and cloudy conditions. Note that the data used are only from occasions when observations and models agree on the presence of clouds.

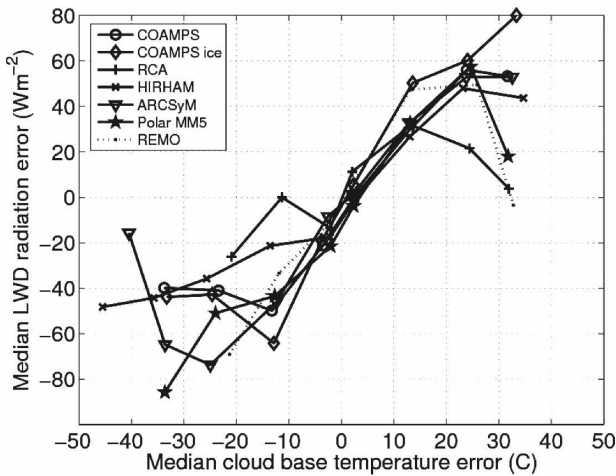


FIG. 15. Error of downwelling longwave radiation (W m^{-2}) as a function of the cloud-base temperature error ($^{\circ}\text{C}$) during summer.

trast to previous comparisons, however, these results consider only cases where the models and the observations agree on the presence of clouds. Moreover, for solar radiation we also require the sun to be more than 10° above the horizon. This reduces the number of cases to evaluate, especially for cloud-free conditions in summer, which are scarce. For the winter we found about 300 and 200 3-h periods where the models correctly simulated the presence and absence of clouds, respectively. The corresponding numbers for summer are 500–600 cases with clouds present and only about 100 with clouds absent; these numbers are slightly different for shortwave and longwave radiation, depending on the available observations, and vary somewhat between the models depending on their performance. The relative lack of data for cloud-free conditions in summer may give rise to more uncertain statistics for clear compared to cloudy conditions and an unfair comparison. This could be remedied by randomly subsampling the cloudy data, but at the expense of statistical quality.

For summer shortwave radiation (Fig. 14a), the PDFs show a significant variability, $\sigma = \pm \sim 100 \text{ W m}^{-2}$, with mostly negative peaks especially for cloudy conditions. For clear conditions, the model ensemble average PDF peaks at $\sim -15 \text{ W m}^{-2}$, although each model has a unique PDF shape. Polar MM5 and ARCSYM have peaks at positive values; both COAMPS runs and REMO have negative peaks and HIRHAM has a wide PDF without a significant peak. For cloudy conditions, the model-ensemble median error is larger, at about -30 W m^{-2} , but although the error PDF tails are slightly longer, the width of the peaks for the different models are narrower ($\sigma = \pm \sim 70 \text{ W m}^{-2}$) and more consistent among models.

A similar pattern occurs for summer longwave radiation (Fig. 14b). The model ensemble average PDFs for clear and cloudy conditions peak at $\sim -20 \text{ W m}^{-2}$ and -15 W m^{-2} , respectively. The intermodel scatter for clear conditions is larger than for cloudy conditions, although the variability for each model's PDF is about the same, $\sigma = \pm \sim 25 \text{ W m}^{-2}$. RCA and REMO systematically overestimate clear-sky longwave radiation and Polar MM5 and COAMPS underestimate it; ARCSYM and HIRHAM have PDF peaks closest to 0.

Thus, in general, there is a deficit in downwelling radiation during summer. Somewhat surprisingly, the intermodel differences are the smallest for cloudy conditions, although some of the larger variability for cloud-free conditions may be due to undersampling. The systematic underestimation of the downwelling longwave radiation under cloudy skies in all models is surprising in view of the preference for low clouds in the Arctic summer. Most of the radiation should come from a cloud base that has a relatively well-constrained temperature, at least through the melt season when the surface temperature seldom deviates from -2 to 0°C , imposed by melting snow and ice (Tjernström et al. 2004). It is also surprising that both shortwave and longwave radiation are biased low. If the modeled clouds were too optically thick but otherwise correctly simulated, one would expect a negative bias in shortwave radiation. However, the longwave radiation would not necessarily have to be in error; it could even have a positive bias depending on the temperature profile and total optical thickness. Figure 15 shows the median error in downwelling longwave radiation as a function of the error in cloud-base temperature, interpolated from the model data and soundings regardless of errors in cloud-base height. Although the actual scatter is significant, it is obvious that a substantial part of the longwave radiation error can be explained by errors in cloud-base temperature. A negative bias in cloud-base temperature could result either from overpredicted cloud base heights or from underpredicted atmospheric temperatures. Because the results (Fig. 4) suggest that the modeled cloud bases are, if anything, too low, a temperature bias is a more likely cause. Such a bias was also found by TEA05; evaluated against soundings, modeled summer temperatures were biased low by up to 2°C below a few hundred meters (see their Fig. 16a).

For the longwave radiation during the winter half of the year (Fig. 14c), the situation is dramatically different. Here the error for clear cases shows a relatively small scatter, $\sigma = \pm 10 \text{ W m}^{-2}$, around an only slightly negative peak. For the cloudy cases, however, there is a significant underestimation of longwave radiation in all models as well as greater intermodel differences.

The model ensemble average PDF has a median around $\sim -30 \text{ W m}^{-2}$, with $\sigma = \pm 25 \text{ W m}^{-2}$, and a long tail down to $\sim -100 \text{ W m}^{-2}$. The reason for this behavior becomes clear when reexamining the time series of LWP in Fig. 8a, which shows a lack of liquid water in winter clouds. Clearly, this issue contributes adversely to the surface radiation balance in winter. Preliminary case study modeling results from the Mixed-Phase Arctic Cloud Experiment (M-PACE) (Prenni et al. 2007) suggest that failures to produce sufficient liquid water are a consequence of applying parameterizations for ice-forming nuclei (IFN) that are based on midlatitude observations. The liquid water presence in Arctic clouds is apparently critically sensitive to the number of IFN, which seems to be systematically lower in the Arctic atmosphere than elsewhere. Prenni et al. (2007) show that by adjusting the parameterization to produce IFN concentrations in line with observations, models are better able to sustain liquid water.

Finally, Fig. 16 summarizes the cloud–radiation interaction for the different models. Figure 16a shows the adjusted surface shortwave radiation as a function of total CWP for all models and observations. The adjusted radiation is defined as the actual surface shortwave radiation divided by the cosine of the solar zenith angle θ . Only cases where $\theta < 80^\circ$ are used to exclude cases that have strong edge effects (with solar radiation reaching the surface slantwise through holes in clouds or being reflected at the edges of cloud holes). Although this very simplistic analysis does not cover all aspects of cloud attenuation of solar radiation, a comparison to observations under the same conditions can be performed. All models overestimate the attenuation for low CWP. For larger CWP, the models group into three categories: REMO, HIRHAM, and Polar MM5 significantly overestimate attenuation of solar radiation and the other models (except COAMPS) are scattered around the observations. COAMPS has a unique behavior with a much weaker dependence on CWP, resulting in overestimated attenuation for thinner clouds and an underestimated attenuation for thicker clouds.

Similarly, the longwave cloud–radiation interaction is illustrated in Fig. 16b. Here we use the apparent sky emissivity, defined as the downwelling longwave radiation divided by the blackbody radiation with respect to the 2-m temperature, to normalize out seasonal differences. Many models (both COAMPS runs, Polar MM5, RCA, and ARCSYM) have a too low apparent emissivity for thin clouds, approaching cloud-free conditions. For COAMPS and RCA, this error is also present for denser clouds, but Polar MM5 and ARCSYM overestimate the apparent emissivity at high CWPs. HIRHAM and REMO agree well with observations;

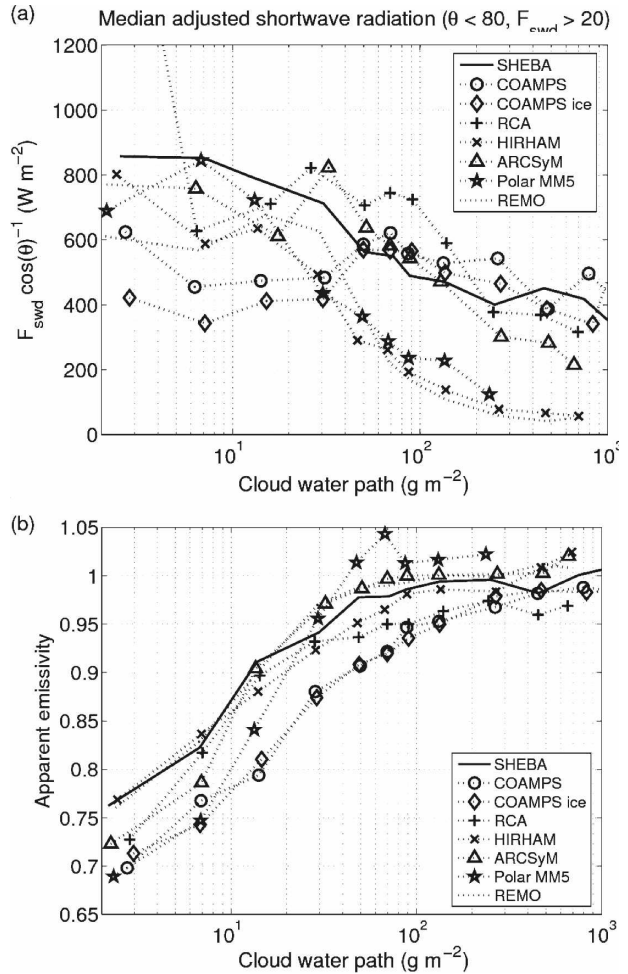


FIG. 16. Normalized influence of clouds on surface radiation: (a) median of the downwelling shortwave radiation (W m^{-2}) divided by the cosine of the solar zenith angle and (b) median of the downwelling longwave radiation divided by the blackbody radiation with respect to the 2-m temperature, both as a function of total CWP (g m^{-2}) for all the models and the observations.

both are indistinguishable from the observations at the 95% level (using a double-sided Student's *t* test, not shown).

4. Conclusions

This study considers errors in surface radiation in six regional models participating in the ARCMIP first experiment as a starting point. Previous studies (Rinke et al. 2006) showed that the large-scale properties in these simulations are well constrained by the lateral-boundary forcing. TEA05 showed that although the temporal description of radiation is adequate in terms of correlation to the observations, model radiation fields suffer from systematic biases; here the down-

welling radiation at the surface is found to be consistently biased negative in many of the models. This study thus focuses on the representations of the modeled clouds and relationships to these radiation errors. One important thing to consider in this context is that this study is not a “beauty contest” among models; our emphasis is on finding common features among the models rather than on labeling any particular model as better or worse than any other.

With a few exceptions, the models evaluated here produce reasonable CWP climatologies. However, in direct comparisons to observations, including the temporal behavior, the comparisons are very poor. Given this fact, it is surprising that the correlations between modeled and observed radiation are relatively good (TEA05), suggesting a tuning in the models involving parameters such as cloud fraction and cloud overlap assumptions. Cloud fraction is not a predicted variable but is determined uniquely in different models based on variables like relative humidity and/or cloud water. There are striking differences between how different models vertically distribute cloud water, particularly when considered on a seasonal basis. The main conclusions about the model cloud characterization are the following:

- There is a tendency, common in all models, to overestimate the occurrence of low and geometrically thin clouds. The models often locate the lowest cloud base at their respective lowest vertical grid point. Thus, although a preference for low clouds is in principle supported by the observations, the apparent agreement for the lowest cloud-base heights in several models could be fortuitous, resulting from a location of the lowest model level at around the same level as where the observations indicate the most commonly occurring lowest cloud base. As a consequence, models with higher near-surface resolution consistently have lower lowest cloud-base heights.
- The lowest cloud-top heights are somewhat too low. All models agree on a minimum occurrence of clouds between 1 and 5 km but tend to underestimate the occurrence of high clouds.
- Some models overestimate the occurrence of high CWP, many models underestimate the occurrence of low-to-medium CWP, and most models overestimate the occurrence of low CWP (in some models by as much as a factor of 2).
- Completely clear conditions are almost absent in the models and occur more seldom than in reality.
- Distinguished by phase, the modeled frequencies of high IWP and medium LWP are generally underestimated.

Modeled clouds that are systematically too low and thin, together with an overrepresentation of clouds with lower CWP, suggest an underestimation of cloud attenuation of solar radiation reaching the surface. The low bias for lowest cloud-base heights would likewise imply a slightly higher downwelling longwave radiation due to warmer cloud-base temperatures, all else being correct. Neither of these expected effects, however, seems to be the case. The story behind the radiation errors is instead one of compensating and overcompensating errors in the models. In summary,

- The negative bias in downwelling longwave radiation at the surface is shown to be a combined effect of model temperature biases in summer (all models except COAMPS are 1–2°C too cold below a few hundred meters; see TEA05) and an almost total lack of liquid water in winter clouds, in contrast to the observations (Intrieri et al. 2002). It is interesting to note that the more advanced models, in the sense of carrying separate prognostic equations for different types of hydrometeors, do not perform better than simpler models with just one single prognostic equation for cloud water.
- For solar radiation, present only in summer, a negative bias is found both for clear and cloudy conditions. For cloudy conditions, model cloud–radiation interactions appear to overestimate the solar attenuation for a given CWP. The source of clear-sky errors may be related to overestimated aerosol attenuation, which may be more characteristic of midlatitude continental conditions.

One might speculate that the model difficulties in characterizing low clouds and the reason for the summer cold bias in many models are related to the models' ability to resolve the “Arctic inversion.” TEA05 evaluated profiles from all these models using the SHEBA soundings. They concluded that the largest errors in the temperature profiles in all seasons were found below about 1 km. Consequently, Tjernström and Graversen (2008, manuscript submitted to *Quart. J. Roy. Meteor. Soc.*), also based on an analysis of SHEBA soundings, found that the main boundary layer inversion in the Arctic is usually below 1 km. These low-level temperature errors were different in different models and for different seasons. TEA05 also speculates, based on the shape of the temperature-bias profiles, that a possible reason for the summer cold bias is an overestimation of low-level cloud-top cooling. A thorough analysis of the ability of the models to resolve the Arctic inversion is beyond the scope of this paper.

We suggest in conclusion that the explanations for model surface radiation errors are partly due to micro-

physics assumptions in the models related to climatological differences in aerosol loading in the Arctic as compared with lower latitudes. Recall that closure assumptions both for the moist physics and for the cloud–radiation interactions largely rely on experimental evidence at lower latitudes. Such impacts are most clearly manifested in the lack, or total absence, of modeled liquid water in cold winter clouds, presumably due to errors in the description of ice nuclei (e.g., Prenni et al. 2007). In a model experiment Prenni et al. (2007) show that excessive IFN concentrations leads to glaciation of cold winter clouds and a subsequent underestimation of downwelling longwave radiation. For summer, we speculate that radiation errors could be caused by overestimated optical thickness for a given CWP over a broad range of CWP values. Fewer aerosols and CCN in the summer Arctic, documented from field experiments (Covert et al. 1996, Heintzenberg et al. 2006), would result in smaller aerosol direct and indirect effects. By not accounting for these effects, the atmospheric attenuation of solar radiation at the surface is overestimated.

Acknowledgments. The authors are grateful to John Cassano, Klaus Dethloff, Colin Jones, Johannes Karlsson, Susanne Pfeifer, Annette Rinke, Tido Semmler, Michael Shaw, Gunilla Svensson, Klaus Wyser, and Mark Žagar for providing the model data used in this study, to Judy Curry and Amanda Lynch for organizing the ARCMIP program, and to Elizabeth Cassano and Jeff Key for setting up forcing data fields for the model simulations. We are also grateful to the SHEBA Atmospheric Flux Group, especially Ola Persson and Chris Fairall, for access to the SHEBA surface observations and to Chris Bretherton and Stefan de Roode for the compilation of SHEBA soundings. This work was partly funded by the European Union 6th Framework program through the DAMOCLES project.

REFERENCES

- Alvarez, R. J., II, W. L. Eberhard, J. M. Intrieri, C. J. Grund, and S. P. Sandberg, 1998: A depolarization and backscatter lidar for unattended operation in varied meteorological conditions. Preprints, *10th Symp. on Meteorological Observations and Instrumentation*, Phoenix, AZ, Amer. Meteor. Soc., 140–144.
- Arctic Climate Impact Assessment, 2005: *Arctic Climate Impact Assessment*. Cambridge University Press, 1042 pp. [Available online at <http://www.acia.uaf.edu/pages/scientific.html>.]
- Cassano, J. J., J. E. Box, D. H. Bromwich, L. Li, and K. Steffen, 2001: Evaluation of Polar MM5 simulations of Greenland's atmospheric circulation. *J. Geophys. Res.*, **106**, 33 867–33 890.
- Christensen, J. H., O. B. Christensen, P. Lopez, E. Van Meijgaard, and A. Botzet, 1996: The HRIHAM4 regional atmospheric climate model. Danish Meteorological Institute Scientific Rep. 96-4, 51 pp.
- Covert, D. S., A. Wiedensohler, P. Aalto, J. Heintzenberg, P. H. McMurry, and C. Leck, 1996: Aerosol number size distributions from 3 to 500 nm diameter in the Arctic marine boundary layer during summer and autumn. *Tellus*, **48B**, 197–212.
- Curry, J. A., and A. H. Lynch, 2002: Comparing Arctic regional climate models. *Eos, Trans. Amer. Geophys. Union*, **83**, 87.
- Hack, J. J., B. A. Boville, B. P. Briegleb, J. T. Kiehl, P. J. Rasch, and D. L. Williamson, 1993: Description of the NCAR Community Climate Model (CCM2). NCAR Tech. Note NCAR/TN-382+STR, 120 pp.
- Harshvardhan, R. Davies, D. A. Randall, and T. G. Corsetti, 1987: A fast radiation parameterization for atmospheric circulation models. *J. Geophys. Res.*, **92**, 1009–1016.
- Heintzenberg, J., C. Leck, W. Birmili, B. Wehner, M. Tjernström, and A. Wiedensohler, 2006: Aerosol number-size distributions during clear and fog periods in the summer high Arctic: 1991, 1996, and 2001. *Tellus*, **58B**, 41–50.
- Hodur, R. M., 1997: The Naval Research Laboratory's coupled ocean–atmosphere mesoscale prediction system (COAMPS). *Mon. Wea. Rev.*, **125**, 1414–1430.
- Holland, M. M., and C. M. Bitz, 2003: Polar amplification of climate change in coupled models. *Climate Dyn.*, **21**, 221–232.
- Hsie, E.-Y., R. A. Anthes, and D. Keyser, 1984: Numerical simulation of frontogenesis in a moist atmosphere. *J. Atmos. Sci.*, **41**, 2581–2594.
- Inoue, J., J. Liu, J. O. Pinto, and J. A. Curry, 2006: Intercomparison of Arctic regional climate models: Modeling clouds and radiation for SHEBA in May 1998. *J. Climate*, **19**, 4167–4178.
- Intrieri, J. M., M. D. Shupe, T. Uttal, and B. J. McCarty, 2002: An annual cycle of Arctic cloud characteristics observed by radar and lidar at SHEBA. *J. Geophys. Res.*, **107**, 8030, doi:10.1029/2000JC000423.
- Jacob, D., 2001: A note to the simulation of annual and interannual variability of the water budget over the Baltic Sea drainage basin. *Meteor. Atmos. Phys.*, **77**, 61–73.
- Jones, C. G., K. Wyser, A. Ullerstig, and U. Willén, 2004: The Rossby Center regional atmospheric climate model. Part II: Application to the Arctic. *Ambio J. Human Environ.*, **33**, 221–227.
- Kattsov, V. M., and E. Källén, 2005: Future climate change: Modeling and scenarios for the Arctic. *Impacts of a Warming Arctic: Arctic Climate Impact Assessment*, C. Symon, Ed., Cambridge University Press, 99–150.
- Lynch, A. H., W. L. Chapman, J. E. Walsh, and G. Weller, 1995: Development of a regional climate model of the western Arctic. *J. Climate*, **8**, 1555–1570.
- MacBean, G., 2005: Arctic climate: Past and present. *Impacts of a Warming Arctic: Arctic Climate Impact Assessment*, C. Symon, Ed., Cambridge University Press, 21–60.
- Mlawer, E. J., S. J. Taubman, P. D. Brown, M. J. Iacono, and S. A. Clough, 1997: Radiative transfer for inhomogeneous atmospheres: RRTM, a validated correlated-*k* model for the longwave. *J. Geophys. Res.*, **102**, 16 663–16 682.
- Moran, K. P., B. E. Martner, M. J. Post, R. A. Kropfli, D. C. Welsh, and K. B. Widener, 1998: An unattended cloud-profiling radar for use in climate research. *Bull. Amer. Meteor. Soc.*, **79**, 443–455.
- Overpeck, J. T., and Coauthors, 2005: Arctic system on trajectory to new, seasonally ice-free state. *Eos, Trans. Amer. Geophys. Union*, **86**, 309–313.
- Persson, P. O. G., C. W. Fairall, E. L. Andreas, P. S. Guest, and

- D. K. Perovich, 2002: Measurements near the Atmospheric Surface Flux Group tower at SHEBA: Near-surface conditions and surface energy budget. *J. Geophys. Res.*, **107**, 8045, doi:10.1029/2000JC000705.
- Prenni, A. J., and Coauthors, 2007: Can ice-nucleating aerosols affect Arctic seasonal climate? *Bull. Amer. Meteor. Soc.*, **88**, 541–550.
- Rasch, P. J., and J. E. Kristjánsson, 1998: A comparison of the CCM3 model climate using diagnosed and predicted condensate parameterizations. *J. Climate*, **11**, 1587–1614.
- Reisner, J., R. M. Rasmussen, and R. T. Bruintjes, 1998: Explicit forecasting of supercooled liquid water in winter storms using the MM5 mesoscale model. *Quart. J. Roy. Meteor. Soc.*, **124**, 1071–1107.
- Rinke, A., and Coauthors, 2006: Evaluation of an ensemble of arctic regional climate models: Spatiotemporal fields during the SHEBA year. *Climate Dyn.*, **26**, 459–472, doi:10.1007/s00382-005-0095-3.
- Roeckner, E., and Coauthors, 1996: The atmospheric general circulation model ECHAM-4: Model description and simulation of present-day climate. Max-Planck Institut für Meteorologie Rep. 218, 90 pp.
- Rutledge, S. A., and P. V. Hobbs, 1983: The mesoscale and microscale structure and organization of clouds and precipitation in midlatitude cyclones. VIII: A model for the “seeder-feeder” process in warm-frontal rainbands. *J. Atmos. Sci.*, **40**, 1185–1206.
- Sass, B. H., L. Rontu, H. Savijärvi, and P. Räisänen, 1994: HIRLAM-2 radiation scheme: Documentation and tests. HIRLAM Tech. Rep. 16, 43 pp.
- Serreze, M., and J. A. Francis, 2006: The Arctic amplification debate. *Climatic Change*, **76**, 241–264, doi:10.1007/s10584-005-9017-y.
- Shupe, M. D., and J. M. Intrieri, 2004: Cloud radiative forcing of the Arctic surface: The influence of cloud properties, surface albedo, and solar zenith angle. *J. Climate*, **17**, 616–628.
- , T. Uttal, and S. Y. Matrosov, 2005: Arctic cloud microphysics retrievals from surface-based remote sensors at SHEBA. *J. Appl. Meteor.*, **44**, 1544–1562.
- , S. Y. Matrosov, and T. Uttal, 2006: Arctic mixed-phase cloud properties derived from surface-based sensors at SHEBA. *J. Atmos. Sci.*, **63**, 697–711.
- Solomon, S., D. Qin, M. Manning, Z. Chen, M. Marquis, K. B. Averyt, M. Tignor, and H. L. Miller, Eds., 2007: *Climate Change 2007: The Physical Science Basis*. Cambridge University Press, 996 pp.
- Stainforth, D. A., and Coauthors, 2005: Uncertainty in predictions of the climate response to rising levels of greenhouse gases. *Nature*, **433**, 403–406.
- Taylor, K. E., 2001: Summarizing multiple aspects of model performance in a single diagram. *J. Geophys. Res.*, **106**, 7183–7192.
- Tjernström, M., C. Leck, P. O. G. Persson, M. L. Jensen, S. P. Oncley, and A. Targino, 2004: The summertime Arctic atmosphere: Meteorological measurements during the Arctic Ocean Experiment 2001. *Bull. Amer. Meteor. Soc.*, **85**, 1305–1321.
- , and Coauthors, 2005: Modelling the Arctic boundary layer: An evaluation of six ARCMIP regional-scale models using data from the SHEBA project. *Bound.-Layer Meteor.*, **117**, 337–381, doi:10.1007/s10546-004-7954-z.
- Uttal, T., and Coauthors, 2002: Surface Heat Budget of the Arctic Ocean. *Bull. Amer. Meteor. Soc.*, **83**, 255–276.
- Wyser, K., and Coauthors, 2008: An evaluation of Arctic cloud and radiation processes during the SHEBA year: Simulation results from eight Arctic regional climate models. *Climate Dyn.*, **30**, 203–223.